Effects of electronic correlation, physical structure, and surface termination on the electronic structure of V_{2}O_{3} nanowires

Amanda L. Tiano, Jing-bin Li, Eli Sutter, Stanislaus S. Wong, and M.-V. Fernández-Serra

Phys. Rev. B **86**, 125135 — Published 26 September 2012

DOI: 10.1103/PhysRevB.86.125135

Effects of Electronic Correlation, Physical Structure, and Surface Termination on the Electronic Structure of V_2O_3 Nanowires

Amanda L. Tiano,[1] Jingbin Li,[2] Eli Sutter,[3] Stanislaus S. Wong,[1,4,*] and

M.-V. Fernández-Serra[2,*]

[1]Department of Chemistry, State University of New York at Stony Brook,

Stony Brook, New York 11794-3400, USA

[2]Department of Physics and Astronomy and the New York Center for Computational Science,

State University of New York at Stony Brook, Stony Brook, NY 11794-3800, USA

[3]Center for Functional Nanomaterials, Building 735, Brookhaven National Laboratory,

Upton, NY 11973, USA

[4]Condensed Matter Physics and Materials Science Department, Building 480,

Brookhaven National Laboratory, Upton, NY, 11973, USA

*Email: maria.fernandez-serra@stonybrook.edu, stanislaus.wong@stonybrook.edu

Abstract

We report a density functional theory (DFT) study of the electronic structure of V_2O_3 in both bulk and nanowire form. In particular, our study is focused on the role of spin polarization and electronic correlations, as computed within the local (spin) density approximation (L(S)DA) and the LDA+U formalism. As expected for a mean-field approach such as DFT, our optimized bulk V_2O_3 structure is shown to be metallic in nature, while an adequate choice of the Hubbard U parameter (U = 4 eV) is enough to open the band gap, making the system insulating. However, this formalism predicts a non-magnetic insulator, as opposed to the experimentally observed anti-ferromagnetic structure, to be the ground state. The electronic structure nature of the V_2O_3 nanowire system is much more complex, and it is strongly dependent on the surface termination of the structures. Our results show that non-spin polarized LDA calculations of <001> grown nanowires are metallic in nature. However, LSDA predicts some surface terminations to be half-metals, with a large band gap opening for one of the spins. When LSDA+U was used to study the nanowire model with a closed-shell oxygen surface termination, we observe insulating behavior with no net magnetic moment, with a 104 meV band gap. This is consistent with the experimentally observed gap recently reported in the literature for similar wires. To experimentally address the surface structure of these nanowires, we perform surface specific nano-Auger electron spectroscopy (AES) on as-synthesized V_2O_3 nanowires. Our experimental results show a higher O: V peak ratio (1.93: 1) than expected for pure V_2O_3, thereby suggesting a higher oxygen content at the surface of the nanowires. From our results, we conclude that oxygen termination is likely the termination for our as-synthesized V_2O_3 nanowires.

I. Introduction

As technology advances, the demand for miniaturization continues to amplify, driving the need for the fabrication of device components measuring on the order of nanometers. However, within this size range, quantum mechanics begins to play a more prominent role, one which can neither be ignored nor considered lightly. Not surprisingly, research has aimed toward the active manipulation of spin degrees of freedom, otherwise known as spintronics, in order to create the next generation of electronics.[1, 2] As such, to achieve the spin-polarization required for spintronics, a great deal of interest has focused on half-metals, which are conductive in one spin orientation, while insulating (or semiconducting) in the other spin orientation.[3, 4] With the goal of producing viable nanoscale devices, half-metals that are low-dimensional in morphology are highly desirable, due to a decrease in the surface reconstructions and corresponding changes to states near the Fermi level that can lead to the destruction of the half-metallic behavior of the intended system. As such, numerous theoretical and experimental investigations have been conducted to determine feasible systems for spintronics applications.

One-dimensional (1D) nanostructures are one of the most commonly explored nanoscale morphologies and their inherent structural anisotropy can lead to unique and interesting optoelectronic and transport properties. In addition, many of these prospective systems contain vanadium, such as vanadium organometallics,[5-7] chalcogenides,[8] VO_x,[9] VO_2,[10] and V-doped systems.[11-13] Interestingly, vanadium-containing systems, especially the family of vanadium oxides, are notorious for possessing complex electronic structures, thereby giving rise to a wide range of attractive magnetic, electronic, opto-electronic, and electrochromic properties.[14, 15] Recently, one of our groups synthesized V_2O_3 nanorods, measuring approximately 64 nm in diameter, which, upon further characterization, revealed interesting transport data. Specifically,

the as-synthesized nanorods exhibited semiconducting behavior from 80 K to 300 K, which had not been reported previously for their bulk counterparts. At room temperature, the nanorods display metallic-like behavior which is similar to what is expected for bulk V_2O_3. Hence, we concluded that our V_2O_3 nanorods possess a small band gap of about 25 meV, given the observed semiconducting behavior at low temperatures and the metallic-like behavior at temperatures at or above room temperature. Thus, our motivation was to investigate the nature of this electronic behavior for 1D nanoscale V_2O_3 and to draw conclusions for other analogous 1D vanadium oxides, so as to explore the applicability of this family of materials for spintronics devices.

Of the family of vanadium oxides, vanadium sesquioxide (V_2O_3) has drawn significant attention because it also exhibits two metal-to-insulator transitions (MIT), which are considered as classic examples of Mott transitions.[16] Initially, at room temperature, V_2O_3 is a paramagnetic metal (PM) but upon cooling, changes to an antiferromagnetic insulator (AFI) at T_N = 168 K. Moreover, it can undergo a transition to a paramagnetic insulator (PI) phase upon doping with either chromium or aluminum, or by varying pressure.[17, 18] Along with the metal-to-insulator transition from PM-AFI, V_2O_3 undergoes a structural transformation. Specifically above T_N, it exhibits the corundum-type structure (space group $R\bar{3}c$)[19] and below T_N, V_2O_3 converts to a monoclinic structure (space group *I2/a*).[20] Arising from its magnetic, electronic, and structural transitions, the applications of vanadium sesquioxide can be expanded so as to include conductive polymer composites, temperature sensors, and current regulators.[21, 22]

Despite the large interest in V_2O_3, as demonstrated by the vast literature available, there is a lack of fundamental understanding in the scientific community with respect to the

complexity of its electronic structure. Following the principles of crystal field theory, V_2O_3 was long considered to be a textbook example of the quintessential one-band Mott-Hubbard system.[23-27] However, more recent theoretical studies have challenged the validity of the conventional one-band Hubbard model in fully and accurately describing the electronic structure of V_2O_3.[28-31] Complementary experimental results[32] have supported the notion of the inadequacies of the Hubbard model for V_2O_3. Hence, attempts have been made in order to construct new models which can more correctly describe the electronic structure.[33-35] The most significant advances have been made with respect to the application of dynamical mean-field theory (DMFT) to the LDA[36] treatment of V_2O_3.[37-41] Similarly, L(S)DA + U methods[4] are also commonly used as a viable approach to studying complex oxide systems containing either transition or rare-earth metals.[2, 3, 7, 11] Inclusion of the electron Coulomb repulsion component, *U*, allows for more accurate investigations of the strong correlation effects present in these types of systems, as has been previously shown by Kresse *et al*. for the bulk V_2O_3 system.[42] Even with recent computational advances in theoretical methods, the available reports of electronic structure investigations using density functional theory (DFT) methods for bulk V_2O_3 are relatively few. To the best of our knowledge, within the family of vanadium oxides, only nanotubes of VO_2 [43] and V_2O_5 [44] have been investigated, and there have not been any theoretical analyses conducted on the precise effect of shrinking V_2O_3 to the nanoscale regime.

Herein, to address these concerns, we have performed computational investigations on both the structural and surface termination effects on the electronic structure of 1D corundum-type V_2O_3 nanowires. The goal of our study has been two-fold. On the one hand, we aim to re-analyze the electronic structure of bulk V_2O_3 using a basis set of localized atomic orbitals, as well as including spin polarization and electronic correlations (within the LDA+U formalism) in

our calculations. This first part (**I**) of our work therefore will serve as a validation of our method. In the second part (**II**), we would like to characterize the electronic structure of V_2O_3 nanowires as a function of their surface termination in order to interpret our previous experimental results and to investigate their potential as candidates for spintronic applications.[45]

II. Theoretical Methodology and Constructs

Electronic structure calculations were conducted using density functional theory (DFT) methods[46, 47] within the local density approximation (LDA) for both bulk and nanowire vanadium oxide systems using a basis set of strictly localized atomic orbitals to expand the Kohn-Sham eigenstates, as implemented in the SIESTA code.[48] We use a double-ζ polarized basis set and Troulier-Martin norm conserving pseudopotentials.[49] Structural information for the bulk V_2O_3 system was taken from crystallographic data provided by Robinson and has been ascribed to the corundum-type structure (Figure 1),[50] which is similar to the crystallographic structure proposed by Dernier.[19] As discussed by Mattheiss,[51] there are two distinctive choices for the unit cells of the V_2O_3 structure: non-primitive hexagonal and primitive rhombohedral. The non-primitive hexagonal cell was used in these calculations and contains 6 formula units, consisting of a total of 30 atoms in the unit cell. We also carried out LDA+U calculations with SIESTA.[63] The LDA+U implementation consists of a simplified rotationally invariant LDA+U formulation[48] coupled with both ferromagnetic and anti-ferromagnetic ordering. Moreover, we also studied the effect of the electric Coulomb repulsion parameter, 'U', in our calculations, varying it from 2.0 to 4.0 eV, given the empirical character of this particular parameter.[47] In the case of spin-polarized calculations, the system was initialized with spin-polarization but with a net magnetic moment of zero, corresponding to a 50: 50 population of spin up and spin down

polarizations at every atom. However, we note that other initial spin configurations were not investigated; therefore the possibility that the results are dependent on the initial spin configuration has not been considered in this work.

Our approach stands in contrast with existing computational literature on V_2O_3, which tends to use the primitive rhombohedral cell. For example, in the work of Mattheiss,[51] V_2O_3 is composed of 2 formula units for a total of 10 atoms within the unit cell. Intrinsically, there is no difference between the two unit cells. However, the computational cost of adding more atoms renders the use of the smaller unit cell as a more convenient choice. Since our unit cell contains 30 atoms, we obtain 3 times more electronic bands in the first Brillouin zone than band structures calculated from the 10 atom unit cell. Brillouin zone integrations were performed using 1050 *k*-points for bulk V_2O_3 within the irreducible hexagonal wedge. For our V_2O_3 nanowire system, the Brillouin zone integration is performed over the range from Γ to X, where $X = \pm \pi/c$, using 150 *k*-points. Calculations on the bulk V_2O_3 structure have been compared with the work of Mattheiss[51] as well as with Eyert *et al.*,[52] since the methods used in this work are similar in nature. We also compared our LDA+U calculation results with the work of Kresse *et al.*.[42]

III. Theoretical Results and Discussion

A. Bulk V_2O_3

i. LDA

We computed the electronic structure of bulk corundum-type V_2O_3, in order to obtain a basis of comparison with V_2O_3 nanowires. Since our methodology was similar to the work of both Mattheiss[51] and Eyert *et al.*,[52] our goal was in producing results for bulk V_2O_3 in good

agreement with both of these prior studies. However, our initial partial V *3d* density of states (DOS), shown in Figure 2 and derived from the bulk V_2O_3 structure of Robinson, did not evince any good separation between the two sets of bands as compared with the previous studies of both Mattheiss[51] and Eyert *et al*.[52] The lattice parameters were systematically varied so as to determine the lowest energy structure using non-spin polarized and subsequently spin polarized calculations. The optimized lattice parameters from LDA calculations are shown in Table 1, along with the crystallographic data obtained from Robinson[50] and Dernier,[19] revealing that the most significant difference is in the '*a'* value for our optimized bulk structure, specifically obtained with the LDA treatment. Differences between theory and experiment can be ascribed both to DFT approximations as well as to the incompleteness of our basis set.

The electronic band structure results from non-spin polarized LDA calculations on the optimized bulk V_2O_3 structure in Figure 3A are shown to be in good agreement with the literature, indicating that the material is metallic in nature, which is an expected result from standard DFT calculations. Moreover, we observe three major sets of bands near the Fermi level (E_F = 0 eV), from -9.1 eV to -3.8 eV (data not shown), from -1.26 eV to 1.4 eV, and from 2.2 eV to 4.7 eV, respectively. The energy ranges for these bands are also consistent with previous electronic structure calculations on V_2O_3. The origin of the first set of bands, which is not shown in Figure 3A, can be attributed to the O *2p* states. The upper two sets of bands are derived from the V *3d* states, specifically the t_{2g} and e_g^{σ} states, respectively, as confirmed by subsequent partial density of states (DOS) calculations (data not shown). In addition, calculations including spin-polarization were conducted on the optimized bulk structure. The results, shown in Figure 3B, are inherently similar to their non-spin counterparts; the electronic bands and DOS maintain the same structure with more bands present.

ii. LDA+ U

LDA+U calculations for bulk V_2O_3 show much better agreement with the experimental values for lattice parameters (see Table 1). This fact can be attributed to the inclusion of on-site Coulomb repulsion, which increases the distance between atoms. We also observed that as 'U' increases, the cell parameter '*a*' increases, while parameter '*c*' decreases, as shown in Table 2. The reason for this observation is that the 'U' correction affects V *3d* π and σ bonds in different ways. As shown in Figure 1, neighboring vanadium atoms in the *ab* plane form a *3d* π bond. As 'U' increases, the strength of π bonds (already weaker than σ bonds) is reduced. Hence, the vanadium atoms move away from each other. Along the *z* axis, strong σ bonding tends to reduce the distance between nearby *ab* layers as the V $3d_{z^2}$ component becomes more localized. Moreover, as 'U' increases, we also observed the separation between the t_{2g} and e_g^{σ} states, as shown in the V *3d* projected DOS (Figure 4A, 4B, and 4C). We conducted additional calculations with antiferromagnetic ordering, wherein neighboring layers perpendicular to the Z-axis are set to possess opposite spins. The PDOS graph of bulk V_2O_3 with antiferromagnetic ordering (Figure 4D) shows a clear band gap, indicating that the antiferromagnetic bulk V_2O_3 structure is an insulator.

iii. LSDA+U

Band structure results from the spin polarized LSDA+U calculations, conducted using spin-polarization with the net unit cell moment set to zero, are shown in Figure 5. These results demonstrate that bulk V_2O_3 is a metal for 'U' values ranging from 2.0 to 3.0 eV. However, it becomes a semiconducting oxide, as we increase the Coulomb potential to 4.0 eV. These data indicate that the large on-site Coulomb repulsion correction substantially reduces hybridization

between the V 3d e_g^{σ} and O *2p* states. We believe that this is the same reason why Kresse's results[47] show bulk V_2O_3 to be a semiconductor. Based on these results, bulk V_2O_3 can be described as a metallic structure with no net magnetic moment in V, and a total energy slightly lower (262 meV/unit cell) than that calculated with antiferromagnetic ordering.

B. V_2O_3 Nanowire

i. *Nanowire Construction*

Since our data for the bulk V_2O_3 are consistent with the literature, thereby validating the methods we have employed, we have constructed our V_2O_3 nanowires using these optimized bulk lattice parameters. Specifically, our nanowires were constructed from the optimized bulk corundum-type V_2O_3 unit cells. The axis of the nanowires is chosen along the *z*-axis, namely the [001] direction, and cut in the *x* and *y*-directions from a central vanadium atom at a chosen radius determined by our desired surface termination. Consistent with the literature on thin films of V_2O_3, there are various surface terminations possible: (i) a half metal V layer, stable under reducing conditions, (ii) a full metal V_2 layer, which is stable under very reducing conditions, (iii) an O_3 layer termination, which is stable in oxygen-rich environments, and (iv) vanadyl (V=O) groups, which have been theoretically shown as the most stable termination over a wide range of oxygen potentials.[53, 54] As such, we have chosen to investigate the latter three surface terminations for our V_2O_3 nanowires shown in Figure 6, and these are referred to as **NW-V** (148 atoms), **NW-O1** (184 atoms), and **NW-O2** (238 atoms), respectively. Further differences in these three nanowire structures will be discussed separately in the sections below, including variables such as composition, radii, bonding, and the chemical state of the surface atoms/ions.

a. NW-V

NW-V was constructed to mimic a full metal layer of vanadium as the nanowire surface termination. First, all three wires have 76 vanadium atoms but vary in composition due to the number of oxygen atoms present. As such, the vanadium terminated surface leaves **NW-V** with 72 oxygen atoms, the least of the three nanowires analyzed. The radius of the as-constructed nanowire was calculated at 5.75 Å. At the surface, the vanadium atoms have varied coordination spheres. They alternate around the circumference of the wire with coordination to either 2 or 3 oxygen atoms, which, under the periodic boundary conditions, act as μ^4 bridging ligands between the metal atoms. As V^{3+} ions, those coordinated to three oxygen atoms are closed-shell and stable. The remaining vanadium ions coordinated to two oxygen atoms are open-shell, but metal-to-metal bonding with the nearest or two nearest vanadium ions yields a closed-shell configuration, and hence, a chemically stable nanowire surface.

b. NW-O1

The second nanowire, **NW-O1**, was constructed with the intention of modeling the O_3 surface termination and has a total of 108 oxygen atoms. The radius of **NW-O1** is slightly larger than that of **NW-V** at 6.09 Å. However, the surface is not composed of O_3 molecules, but rather contains oxygen atoms which are bonded to either 2 or 3 vanadium atoms in bent and trigonal pyramidal geometries, respectively. Again, as with **NW-V**, all oxygen atoms have sufficient bonding to satisfy the O^{2-} ion, making all the oxygen atoms closed-shell. Thus, the surface herein is a chemically stable termination.

c. NW-O2

Lastly, **NW-O2** was constructed as a model for the vanadyl (V=O) group terminated surface and contains 162 oxygen atoms, the most of the three nanowire structures analyzed. The

O: V ratio of **NW-O2** structure is the closest to our experiment data (1.93: 1) among the three structures studied. Since **NW-O2** has the highest number of atoms, it is also significantly larger in the radial direction with a radius of 6.68 Å. Since the surface was designed with the intention of modeling the V=O groups, the surface is composed of oxygens bonded to vanadium atoms. The bond lengths for these groups measure either 1.97 Å or 2.06 Å. The bond length of vanadyl groups has been previously studied and the threshold for the double bond is accepted at lengths shorter than 1.74 Å.[55] Since the bond lengths at the surface are above this maximum value, the groups at the surface of our nanowire consist of singly bonded oxygen atoms, leaving the exposed surface consisting of open-shell oxygen atoms. We can reasonably assume that the **NW-O2** surface is unstable by comparison with the closed-shell V=O groups which we expected to model as the surface termination.

In order to investigate our V_2O_3 nanowires, we independently studied the effect of (1) '*c'*, the unit cell length for the **NW-O2** nanowire structure, (2) surface termination, and (3) structure relaxation on the resulting electronic structures. We should note that we only optimized the value of the '*c'* lattice parameter for **NW-O2** due to large surface stresses which prevented structural relaxation of the nanowires. **NW-V** and **NW-O1** were more structurally stable and hence, relaxation could be accomplished by using the optimized value ('*c'* = 14.07 Å) we had derived for the bulk. All the wire calculations are performed for tetragonal unit cells. Wires are periodic along the '*c'* axis and periodic images are separated by more than 40 Å of vacuum along the directions perpendicular to the wire axis. This unit cell choice hence ensures the effective uni-dimensionality of the calculated wires. Herein, we have discussed the effect of structural relaxations upon the V_2O_3 nanowires. Specifics regarding the effects of the unit cell length and

surface termination on the electronic structure can be found in the Supplementary Information section.

ii. Effect of structural relaxations on electronic structure

Each of the as-constructed nanowires was relaxed to determine the minimum energy geometry and to thereby decrease the system stresses. Specifically, the system was relaxed until the overall forces were less than 0.1 eV/Å. Following the relaxation process, the band structure of the system was calculated for comparison. Only relaxations for **NW-Va** and **NW-O1a** were successful when *'c'* = 14.07 Å; a comparable relaxation for the **NW-O2a** structure was accomplished with an optimized unit cell length of '*c'* = 12.90 Å. This difference in the *'c'* lattice parameter may be a consequence of the presence of initial unstable open-shell oxygen atoms inducing large reconstructions at the surface. Moreover, these relaxations were only achieved with the exclusion of spin-polarization considerations from the calculations. The final structures for all three nanowires are shown in Figure 7 along with the corresponding electronic structures for each. In addition, the data for several parameters for the initial and relaxed structures are shown in Table 3.

a. NW-V

The resulting structure for the vanadium surface terminated nanowire in Figure 7 is very different from the initial construction, shown in Figure 6. In fact, the surface atoms have compressed the nanowire in the *xy* direction, resulting in a narrower wire, with a radius of 5.23 Å as compared with the initial radius of 5.75 Å, translating to about a 10% decrease in size. Additionally, the oxygen atoms closest to the surface in the initial as-constructed structure are now physically closer together and even protrude outwards from the surface of the nanowire.

This situation may suggest that the structure would be more stable with the oxygen atoms residing at the surface. In addition to lowering energy, the stresses within the system are in fact decreased upon relaxation. Closer analysis shows that the presence of vanadium atoms at the surface leads to a high total surface charge. While the vanadium atoms at the surface maintain a chemically stable closed-shell configuration, these data are consistent with the idea of this type of surface termination as being quite structurally unstable, in agreement with the idea of the reconstruction of the nanowire system during relaxation, leading to a net movement of oxygen atoms to the surface.

The resulting band structure for **NW-V** (Figure 7) also shows a dramatically different structure as compared with that of the previous set of calculations (Supplementary Figure S1 and S2). The nanowire is clearly semiconducting in nature with an indirect band gap around the Fermi level of ~ 9 meV, with very few bands present around the Fermi level. Moreover, what is apparent in Figure 7 is the lack of symmetry present in the final relaxed structure. It is clear that one side of the nanowire is more compressed than the other in the *x* and *y* directions. This lack of symmetry causes the opening of some small gaps, which appear as a result of the formation of discrete bands in the electronic structure plots. Moreover, the electronic structure of **NW-V** is very distinctive by comparison with the optimized bulk V_2O_3 structure, as there are many differences present in the electronic structures in Figure 7 and Figure 3, respectively. Although there is a dominant contribution from vanadium around the Fermi level, which is similar to bulk V_2O_3, we believe that the semiconducting behavior observed in the electronic structure data for **NW-V** is a consequence of the rearrangement of the oxygen atoms towards the surface and their interaction with the V atoms. Thus, as we will see with **NW-O1**, the surface plays a crucial role in determining the ensuing electronic behavior of V_2O_3 nanowires.

b. NW-O1

As with **NW-V**, following relaxation, the core of the nanowire structure in **NW-O1** is compressed towards the center. This is confirmed by the decrease in radius from 6.09 Å to 5.63 Å after relaxation, which corresponds to a 7.6% radial decrease. However, this structure is dramatically different in that the oxygen atoms on the surface appear to be expanding out from the center, forming a more pyramidal or bent geometry, thereby causing them to protrude further from the core of the nanowire. Additionally, Table 3 shows that the surface charges for **NW-O1** are also significantly lower by comparison with **NW-V**, an observation emphasizing the stability of the V_2O_3 nanowire comprised of O-terminated surfaces.

In the analysis of the electronic structure of **NW-O1**, it is clear that this wire also results in a very different electronic structure from that of as-constructed nanowires, and rather closely resembles the relaxed **NW-V** electronic structure. Figure 7 shows that the relaxed **NW-O1** structure also yields a small indirect semiconducting gap present around the Fermi level of ~ 3.2 meV. Moreover, the bands present around the Fermi level appear to be discrete from one another, likely an outcome of symmetry breaking to a similar extent that was observed for **NW-V**, as evidenced by the relatively larger gaps in the electronic structure for **NW-O1**. Since the oxygen atoms contribute very little to the electronic structure in this range, the observed semiconducting gap can clearly be ascribed to a lack of electronic states from the vanadium atoms. One question still to be addressed is whether the origin of the band gap is symmetry induced or if it is a pure intrinsic effect, associated with the surface termination and reconstruction of this nanowire. We believe that the oxygen surface termination is a necessary condition for achieving semiconducting behavior in the wire. The reason for this assertion is that the bands around the Fermi level of this termination are much less dispersive than V bands. While disorder might play

an effect, this is a surface disorder phenomenon, which is not core-induced, and hence, will be always present in these structures.

c. NW-O2

Consistent with the other two nanowire structures, **NW-O2** is also compressed in the *xy* direction upon relaxation. However, the change is not as drastic as the former two, as evinced by the slight radial decrease (e.g. 2.2 %) from 6.68 Å to 6.53 Å. More importantly, the length of the surface V-O bonds has decreased drastically to 1.59 Å, which is well within the accepted lengths for V=O groups. Thus, we have shown that relaxing the constructed nanowires has produced a more chemically stable surface termination as these bonds now model a closed-shell system. Moreover, the surface charges on the oxygen atoms are similar to those of **NW-O1**.

Analysis of the electronic structure in Figure 7 for the relaxed **NW-O2** structure reveals a drastically different set of bands as compared with that associated with both relaxed structures for **NW-V** and **NW-O1**, as well as with the as-constructed **NW-O2** nanowire shown in Figure 6. Unlike **NW-V** and **NW-O1**, there is no gap around the Fermi level, which clearly evinces a metallic band structure which is highly reminiscent of the electronic structure calculated for the optimized bulk V_2O_3 structure in Figure 3B. Although **NW-O2** is shown to be metallic, the bands around the Fermi level are still dominated by the vanadium atoms. These data reaffirm the importance of the oxygen surface construction about the outer vanadium atoms; in effect, the presence of V = O groups appears to make **NW-O2** metallic in nature.

Based on these results, we can easily conclude that the **NW-O2** surface construction is bulk-like in behavior and is not consistent with our previous experimental data on as-synthesized V_2O_3 nanowires. It is clear that the number and position of the oxygen atoms on the surface play

a critical role in determining the electronic behavior of the V_2O_3 nanowires. The tendency of **NW-V** to move oxygen atoms towards the surface upon relaxation is further evidence of this trend. In fact, the electronic structures of both **NW-V** and **NW-O1** most closely resemble our experimental data, as both model nanowires possess an intrinsic semiconducting gap about the Fermi level. It may be more likely that the structure and surface of **NW-V** are most consistent with our experimental data and reaction conditions, namely the controlled presence of a reducing atmosphere, which would logically result in the formation of a proportionally higher number of vanadium atoms at the surface of our as-synthesized V_2O_3 nanowires. However, as both nanowires structures have undergone surface reconstructions during relaxation processes, resulting in both oxygen terminated surfaces, we can therefore conclude that both **NW-V** and **NW-O1** are viable surface compositions of our as-synthesized nanowires.

iii. LSDA results with relaxed NW-V, NW-O1, and NW-O2 nanowires

In order to investigate the applicability of the V_2O_3 nanowires for spintronics applications, we repeated calculations on our optimized nanowire structures with the inclusion of spin-polarization within the LDA algorithm. The corresponding results are shown in Figure 8. It is clear that all three nanowires are in fact spin polarized, as evidenced by the magnetization values shown in Table 3. By comparison with their non-spin polarized counterparts (Figure 7), the electronic results are drastically different. In the case of **NW-V** and **NW-O1**, the nanowires are shown to be half-metallic in nature. Specifically, the majority spin component is metallic, whereas the minority spin analogue is semiconducting with gaps present near the Fermi level, as evidenced by the DOS results. The **NW-O2** system behaves differently as compared with the other two nanowire systems. In this case, the majority spin component is metallic in nature, but there is no corresponding semiconducting gap present in the minority spin element. However, a

more detailed study of the bands close to the Fermi level from the minority spin scenario shows the potential to have created a gap so as to induce spin-polarization for this nanowire structure. Not surprisingly, all the DOS results have shown that the vanadium atoms heavily dominate the electronic states about the Fermi level, which is an observation consistent with our non-spin polarized calculations on V_2O_3 nanowires.

iv. LSDA+U results with relaxed NW-O2 nanowire

Though the LSDA calculation results of our **NW-O2** nanowire suggest that it is a metal, our experiments predict high O concentration at the nanowire surface. Therefore, we performed LSDA+U calculations on **NW-O2** without magnetic ordering. We chose 'U' to be 3.43 eV, the same value used by Kresse *et al*.[42] Our calculation results show *'c'* = 13.53 Å for the optimized structure, which is 0.63 Å larger than the optimized parameter, *'c'* = 12.9 Å, derived from LSDA calculations. Within the LSDA formalism, the surface O atom (see Figure 6.3) forms very strong bonds with neighboring V atoms with bond lengths of 1.69 Å, as these are consistent with vanadyl (V = O) bond lengths.[55] These V-O bonds pull nearby *ab* vanadium planes closer to each other, which explains why the NW-O2 results possess a smaller *'c'* value than NW-V and NW-O1.

As discussed previously in the bulk LSDA+U section, including an on-site Coulomb repulsion correction substantially reduces hybridization between the V *3d* e_g^{σ} and O *2p* states, thereby increasing the surface V-O bond length to 2.06 Å, which in turn increases the unit cell length in z direction. The band structures, as shown in Figure 9A and B, show that small band-gaps are present. Specifically, the majority spin has a ~ 104 meV gap, while the minority spin

has a 2.047 eV gap (see Table 3). These results agree very well with our experimental observation that the nanowire is semiconducting in nature.

IV. Surface Experimental Verification of Theoretical Results

V_2O_3 nanowires were synthesized following a protocol previously developed by one of our groups.[45] First, an aqueous solution of V_2O_5 is mixed with KOH and hydrazine, followed by a pH adjustment to ~ 3 by dropwise addition of HCl. The reaction mixture is hydrothermally treated at 150°C for 48 hours, producing VO_2 nanorods. These as-synthesized VO_2 nanorods are then heated at a ramp rate of 30°C/min to 700°C and subsequently held for 1 hour in a reducing atmosphere (Ar / H_2) to form V_2O_3 nanowires.

Powder samples for X-ray diffraction (XRD) analysis were prepared by forming a slurry via sonication in absolute ethanol (Acros Organics, 99.5+ %), deposited onto glass slides, and dried. The analysis was conducted using a Scintag diffractometer operating in the Bragg configuration using Cu Kα radiation ($\lambda = 1.54$ Å) scanned over a range of 20° to 80° in 2θ with 1° step size. Sample preparation for SEM and nano-Auger electron spectroscopy characterization was conducted by dispersion of the as-prepared product in ethanol followed by evaporation onto a silicon wafer. The morphology and sizes of the final products were investigated using a Hitatchi S-4800 FE-SEM. Nano-Auger electron spectroscopy was performed using an Omicron Nanotechnology system equipped with an ultra-high vacuum (UHV) FE-SEM and Auger electron analyzer, with excitation of the Auger electrons achieved using a focused SEM electron beam (10 keV, 100 pA).

Results

The resulting XRD pattern for the as-prepared sample could be indexed to the corundum-type V_2O_3 (JCPDS # 85-1411) with the space group of $R\bar{3}c$ (Supplementary Figure S3). A corresponding SEM analysis revealed that as-synthesized V_2O_3 possessed a nanowire morphology, as expected. Moreover, the thin V_2O_3 nanowires measured 27 ± 4 nm in diameter and up to several microns in length (Supplementary Figure S4).

In order to compare theoretical results on the surface termination effects with respect to actual experimental data, we probed the nanowire surface with nano-Auger electron spectroscopy to determine elemental composition. Nano-Auger detected the presence of both vanadium (437 and 473 eV) and oxygen (514 eV) on the external nanowire surface (Figure 10),with minor shifts in peak locations observed. However, this is consistent with the difference in the oxidation state of the vanadium in V_2O_3 with respect to pure vanadium.[56] As the sample was stored in a glove box and subsequently moved to the UHV SEM system for analysis, the likelihood of other oxygen-containing adsorbates is significantly decreased, thereby rendering the ratio of the O: V (514: 437 eV) peaks more reliable for stoichiometric measurements. In our spectrum, the intensities of these two peaks were determined to be 1.93: 1, which is slightly higher than the expected value for V_2O_3.[57] Since XRD analysis confirmed the presence of pure V_2O_3 with no impurities, the O: V ratio suggests that there is a higher oxygen content at the surfaces of the nanowires. This experimental observation is in agreement with our theoretical results. Hence, it is highly likely that the as-synthesized V_2O_3 nanowires are oxygen-terminated.

V. Conclusions

In conclusion, we have presented here a detailed study[58] of the electronic and atomic structure of three different surface-terminated V_2O_3 nanowires and performed a detailed comparison with the bulk V_2O_3 system. Our study has paid detailed attention to the role of electronic correlations, as described by the LDA+U approximation. Both spin polarized and non-spin polarized calculations have been performed. We have shown that the electronic structure nature of the V_2O_3 nanowire system is much more complex than its bulk counterpart, and it is strongly dependent on the surface termination of the structures.

Specifically, our results show that non-spin polarized LDA calculations of <001> grown nanowires are metallic in nature. However, LSDA predicts some surface terminations to be half-metals, with a large band gap opening for one of the spins. When LSDA+U was used to study the nanowire model with a closed-shell oxygen surface termination, we observed insulating behavior with no net magnetic moment in V coupled with a 104 meV band gap. This result is consistent with the experimentally observed gap recently reported in the literature for similar wires by one of our groups.[45] In addition, analysis of as-synthesized V_2O_3 nanowires via nano-Auger electron spectroscopy demonstrated a larger O (514 eV): V (437 eV) peak ratio than expected for bulk, suggesting that the oxygen content is higher at the surfaces of the nanowires. We can therefore reasonably conclude that the as-synthesized V_2O_3 nanowires are oxygen-terminated and that this termination is the most stable among all other credible possibilities.

Acknowledgements

MVFS was funded by DOE award number DE-FG02-09ER16052. JBL acknowledges support from MURI award number FA9550-12-1-0038. This research utilized resources at the New York Center for Computational Sciences at Stony Brook University/Brookhaven National Laboratory which is supported by the U.S. Department of Energy under Contract No. DE-AC02-98CH10886 and by the State of New York. Research (including support for A.T. and S.S.W.) was supported by the U.S. Department of Energy, Basic Energy Sciences, Materials Sciences and Engineering Division. Auger experiments in this manuscript were performed at the Center for Functional Nanomaterials located at Brookhaven National Laboratory, which is supported by the U.S. Department of Energy under Contract No. DE-AC02-98CH10886.

Figures/Figure Captions

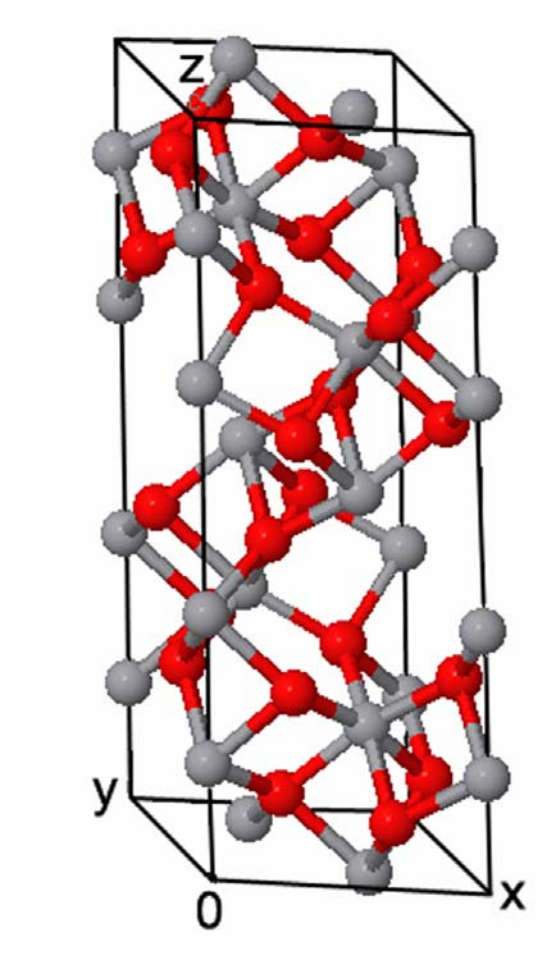

Figure 1. Corundum-type bulk V_2O_3 unit cell with vanadium atoms in grey and oxygen atoms in red.[50]

V_2O_3 unit cell	a (Å)	c (Å)
Robinson	4.9776	13.9647
Dernier	4.952	14.003
Optimized with LDA	4.78	14.07
Optimized with LDA+U (U = 3.43 eV)	4.993	13.872

Table 1. V_2O_3 unit cell parameters for the optimized structures as compared with those of the literature.[19, 50]

U (ev)	a (Å)	c (Å)
2.0	4.942	13.939
3.0	4.971	13.920
4.0	5.021	13.803

Table 2. V_2O_3 unit cell parameters for the LDA + U optimized structure with 'U' = 2.0, 3.0, and 4.0 eV, respectively.

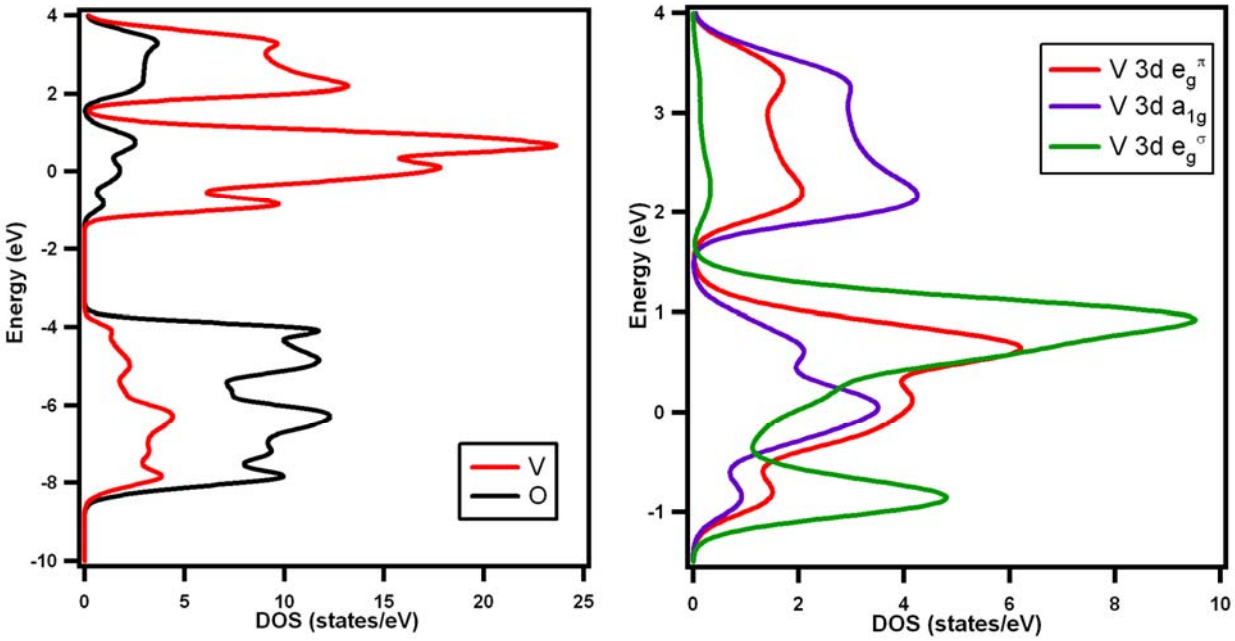

Figure 2. Projected electronic density of states for hexagonal V_2O_3 (left) and partial *V 3d* density of states (right) using crystallographic data provided by Robinson.[50]

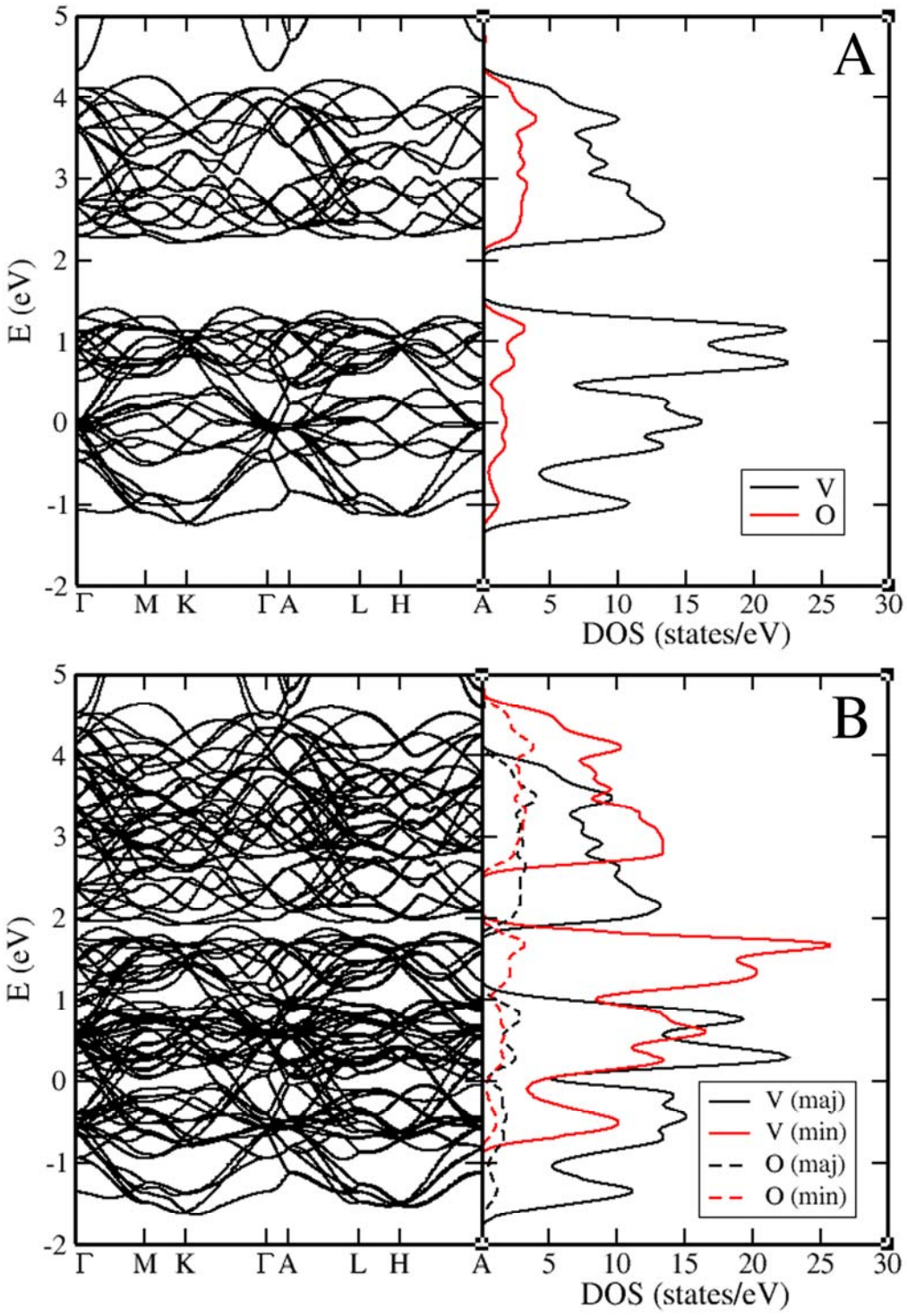

Figure 3. Electronic band structure and corresponding DOS for the optimized bulk V_2O_3 structure both without (A) and with spin-polarization (B).

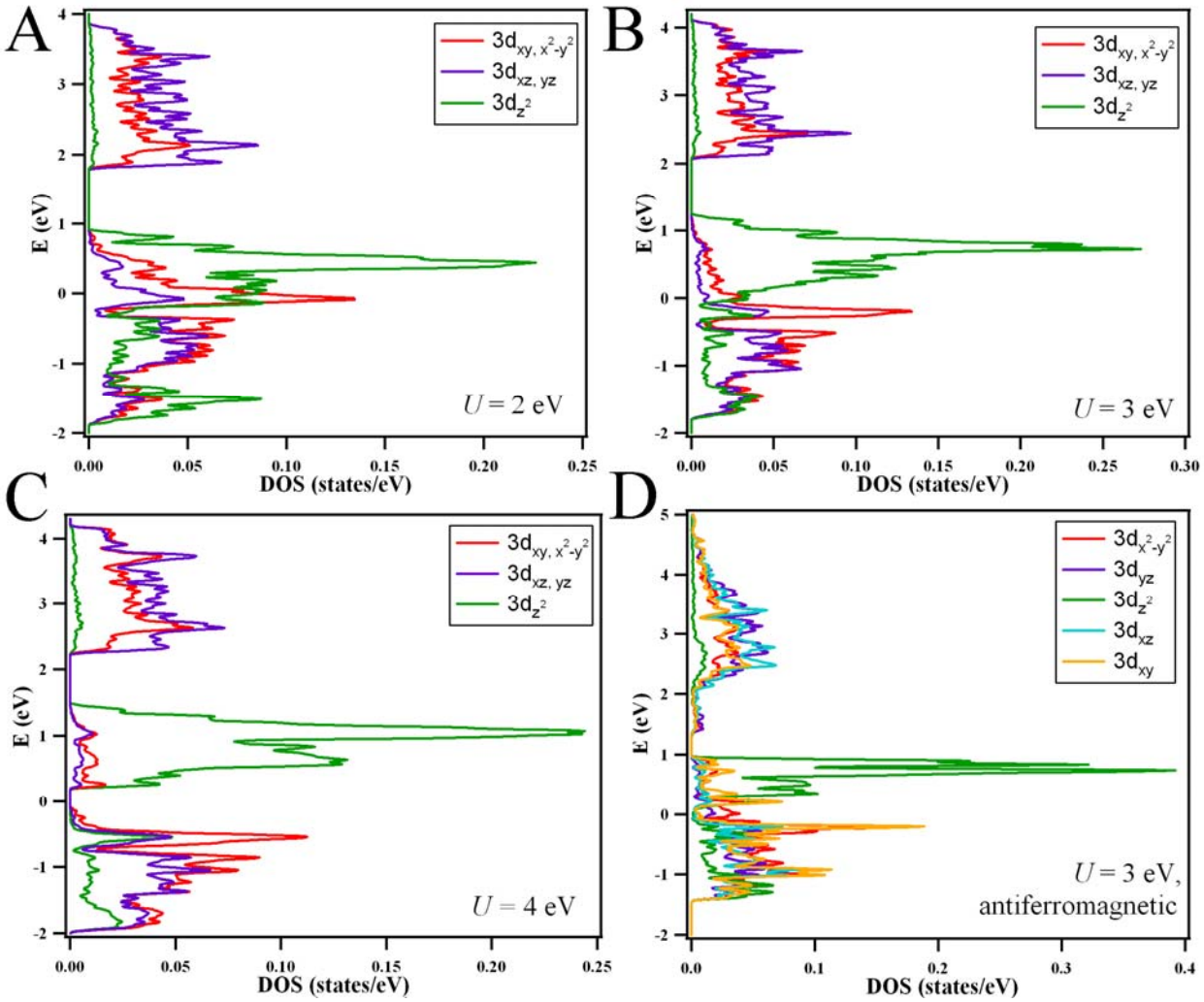

Figure 4. Projected DOS for the optimized bulk V_2O_3 structure with spin-polarized calculations where the net unit cell moment is set to 0 for (A) 'U' = 2 eV, (B) 'U' = 3 eV, (C) 'U' = 4 eV, and (D) anti-ferromagnetic ordering for 'U' = 3 eV.

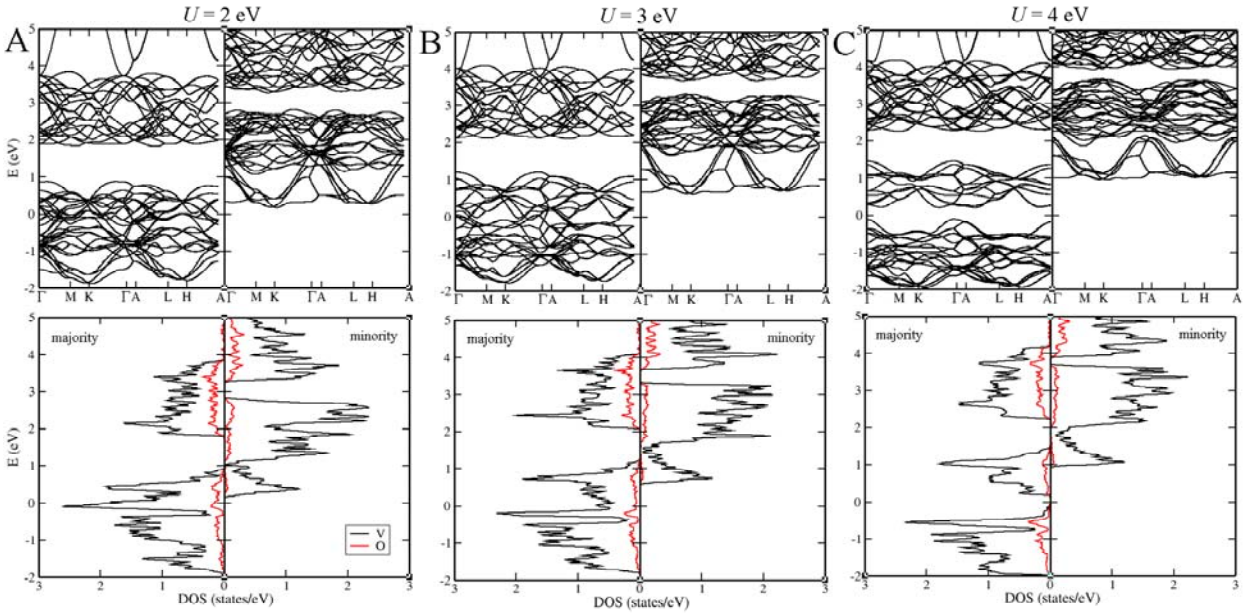

Figure 5. Electronic band structure and the corresponding DOS for the optimized bulk V_2O_3 structure using (A) 'U' = 2.0 eV; (B) 'U' = 3.0 eV; and (C) 'U' = 4.0 eV. Note that all these systems are calculated with the net unit cell magnetic moment set to zero. Densities for vanadium and oxygen are shown as black and red lines, respectively.

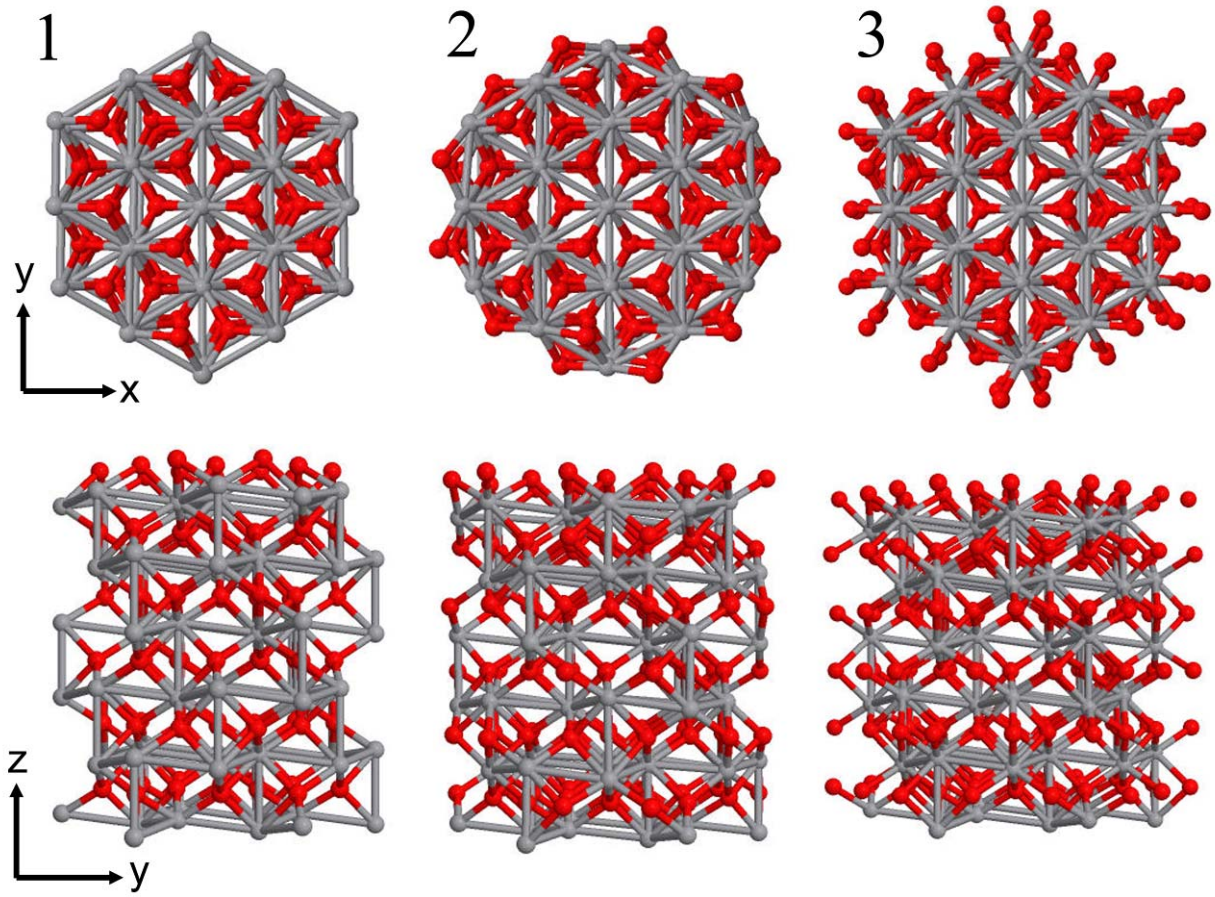

Figure 6. Nanowire surfaces terminated with a single V (1), an O_3 layer (2), and a V=O layer (3), respectively. Vanadium atoms are shown in grey and oxygen atoms are highlighted in red.

Parameter	NW-V	NW-O1	NW-O2	NW-O2 (LSDA + U)
r_i (Å)	5.75	6.09	6.68	6.68
r_f (Å)	5.23	5.63	6.53	6.52
Average surface charge	12.55 per V atom	6.56 per O atom	6.36 per O atom	6.42 per O atom
Magnetization (Q_{up}-Q_{down})	17.1256	151.53	11.8495	56.00
Average bond lengths (Å)				
V-V	2.63 ± 0.33	2.69 ± 0.28	2.88 ± 0.24	2.80 ± 0.21
V-O (bulk)	2.01 ± 0.05	1.97 ± 0.06	1.99 ± 0.24	1.89 ± 0.13
V-O (surface)	1.96 ± 0.11	1.90 ± 0.09	1.69 ± 0.11	2.08 ± 0.21
Band gap (eV)	0.034 (minority)	0.010 (minority)	N/A	0.066 (majority), 2.047 (minority)

Table 3. Various LSDA calculated parameters for **NW-V, NW-O1,** and **NW-O2** (LSDA and LSDA+U) at '*c*' = 14.07 Å, for the as-constructed surface (i) and after relaxation (f).

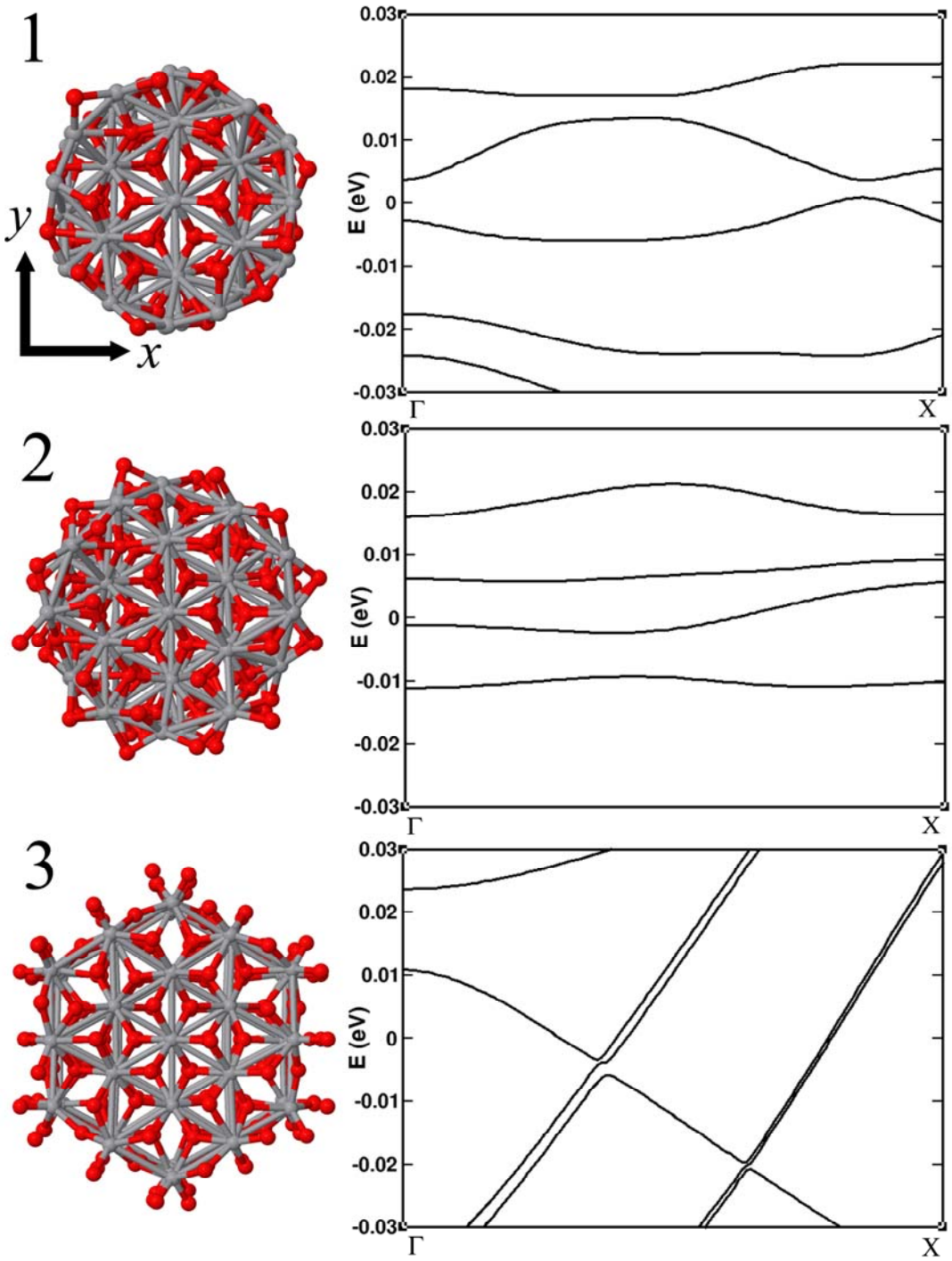

Figure 7. Nanowire structures shown along with the corresponding electronic structure for **NW-V**, **NW-O1,** and **NW-O2** after relaxation without spin-polarization.

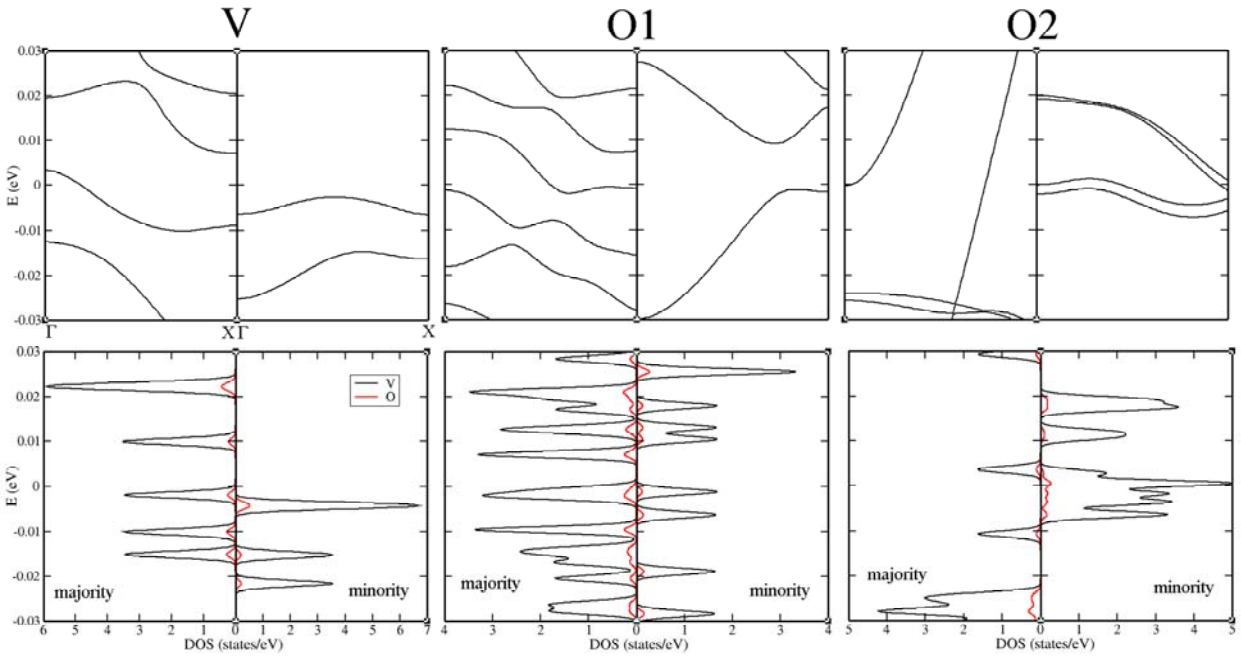

Figure 8. Electronic structure (top) and density of states (DOS, bottom) for **NW-V**, **NW-O1,** and **NW-O2,** calculated using spin-polarization and plotted with respect to both majority and minority spin components. Densities for vanadium and oxygen are shown as black and red lines, respectively.

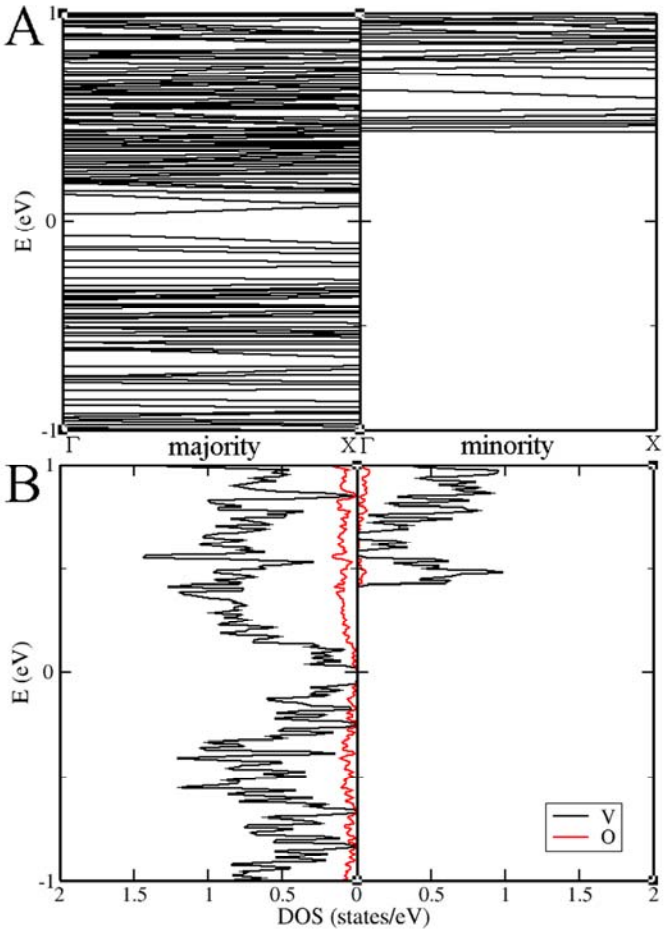

Figure 9. Electronic band structure (A) and corresponding DOS (B) for the V_2O_3 nanowire with the net unit cell magnetic moment set to 0. Densities for vanadium and oxygen are shown as black and red lines, respectively.

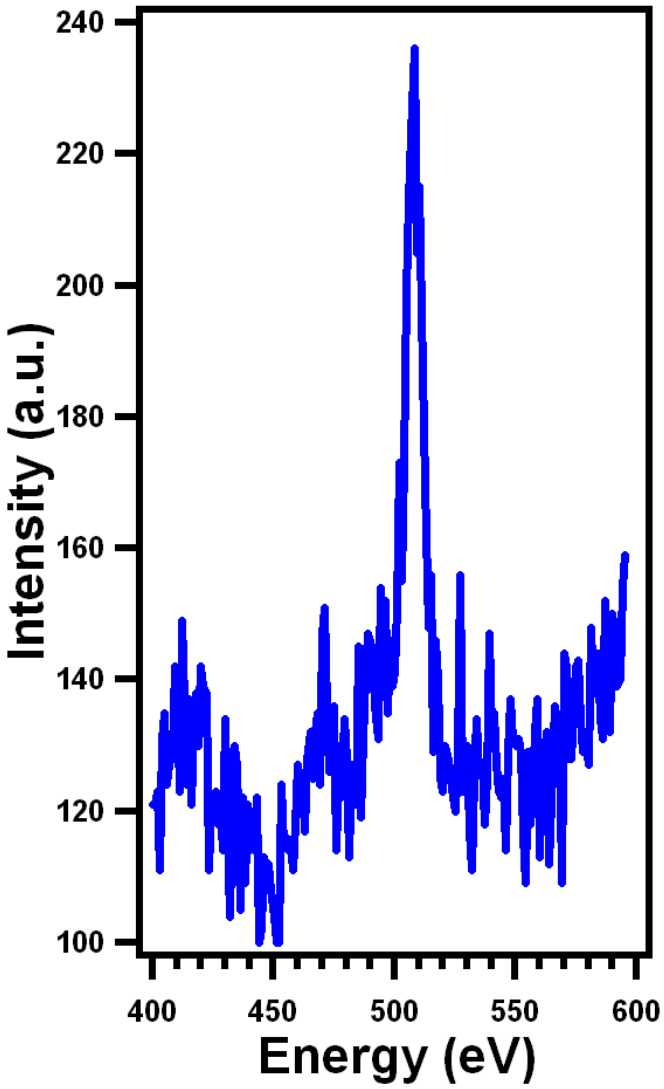

Figure 10. UHV nano-Auger electron spectrum obtained from the surface of a V_2O_3 nanowire, showing the presence of both vanadium (437 and 473 eV) and oxygen (514 eV) peaks.

References

[1] S. A. Wolf, D. D. Awschalom, R. A. Buhrman, J. M. Daughton, S. von Molnar, M. L. Roukes, A. Y. Chtchelkanova, and D. M. Treger, Science **294**, 1488 (2001).

[2] D. D. Cuong, B. Lee, K. M. Choi, H.-S. Ahn, S. Han, and J. Lee, Phys. Rev. Lett. **98**, 115503 (2007).

[3] O. Bengone, M. Alouani, Bl, ouml, P. chl, and J. Hugel, Phys. Rev. B **62**, 16392 (2000).

[4] V. Anisimov, F. Aryasetiawan, and A. I. Lichtenstein, J. Phys.: Condens. Matter **9**, 767 (1997).

[5] S. S. Mallajosyula, P. Parida, and S. K. Pati, J. Mater. Chem. **19**, 1761 (2009).

[6] V. V. Maslyuk, A. Bagrets, V. Meded, A. Arnold, F. Evers, M. Brandbyge, T. Bredow, and I. Mertig, Phys. Rev. Lett. **97**, 097201 (2006).

[7] F. Zhou, C. A. Marianetti, M. Cococcioni, D. Morgan, and G. Ceder, Phys. Rev. B **69**, 201101 (2004).

[8] X. Wen-Hui and L. Bang-Gui, J. Phys.: Condens. Matter **15**, 5085 (2003).

[9] L. Krusin-Elbaum, D. M. Newns, H. Zeng, V. Derycke, J. Z. Sun, and R. Sandstrom, Nature **431**, 672 (2004).

[10] K. West, et al., Journal of Superconductivity and Novel Magnetism **21**, 87 (2008).

[11] C. Loschen, J. Carrasco, K. M. Neyman, and F. Illas, Phys. Rev. B **75**, 035115 (2007).

[12] C.-K. Yang, J. Zhao, and J. P. Lu, Nano Lett. **4**, 561 (2004).

[13] H. Saeki, H. Tabata, and T. Kawai, Solid State Commun. **120**, 439 (2001).

[14] C. V. Ramana, S. Utsunomiya, R. C. Ewing, and U. Becker, Solid State Commun. **137**, 645 (2006).

[15] S. Surnev, M. G. Ramsey, and F. P. Netzer, Prog. Surf. Sci. **73**, 117 (2003).

[16] N. F. Mott, *Metal Insulator Transitions* (Taylor & Francis, London, 1974).

[17] D. B. McWhan, A. Menth, J. P. Remeika, W. F. Brinkman, and T. M. Rice, Phys. Rev. B **7**, 1920 (1973).

[18] D. B. McWhan, J. P. Remeika, T. M. Rice, W. F. Brinkman, J. P. Maita, and A. Menth, Phys. Rev. Lett. **27**, 941 (1971).

[19] P. D. Dernier, J. Phys. Chem. Solids **31**, 2569 (1970).

[20] P. D. Dernier and M. Marezio, Phys. Rev. B **2**, 3771 (1970).

[21] D. M. Moffatt, J. P. Runt, A. Halliyal, and R. E. Newnham, J. Mater. Sci. **24**, 609 (1989).

[22] Y. Pan, G. Z. Wu, and X. S. Yi, J. Mater. Sci. **29**, 5757 (1994).

[23] C. Castellani, C. R. Natoli, and J. Ranninger, Phys. Rev. B **18**, 5001 (1978).

[24] C. Castellani, C. R. Natoli, and J. Ranninger, Phys. Rev. B **18**, 4967 (1978).

[25] C. Castellani, C. R. Natoli, and J. Ranninger, Phys. Rev. B **18**, 4945 (1978).

[26] J. Hubbard, Proc. R. Soc. London, Ser. A **276**, 238 (1963).

[27] J. Hubbard, Proc. R. Soc. London, Ser. A **281**, 401 (1964).

[28] M. S. Laad, L. Craco, and E. Muller-Hartmann, Phys. Rev. B **73**, 045109 (2006).

[29] S. Y. Ezhov, V. I. Anisimov, D. I. Khomskii, and G. A. Sawatzky, Phys. Rev. Lett. **83**, 4136 (1999).

[30] U. Schwingenschlogl, V. Eyert, and U. Eckern, Euro Physics Letters **64**, 682 (2003).

[31] I. S. Elfimov, T. Saha-Dasgupta, and M. A. Korotin, Phys. Rev. B **68**, 113105 (2003).

[32] J. H. Park, L. H. Tjeng, A. Tanaka, J. W. Allen, C. T. Chen, P. Metcalf, J. M. Honig, F. M. F. de Groot, and G. A. Sawatzky, Phys. Rev. B **61**, 11506 (2000).

[33] S. Di Matteo, N. B. Perkins, and C. R. Natoli, Phys. Rev. B **65**, 054413 (2002).

[34] Z. Ropka and R. J. Radwanski, Physica B **378-380**, 301 (2006).
[35] R. Shiina, F. Mila, F. C. Zhang, and T. M. Rice, Phys. Rev. B **63**, 144422 (2001).
[36] K. Held, I. A. Nekrasov, N. Blümer, V. I. Anisimov, and D. Vollhardt, Int. J. Mod Phys B **15**, 2611 (2001).
[37] K. Held, G. Keller, V. Eyert, D. Vollhardt, and V. I. Anisimov, Phys. Rev. Lett. **86**, 5345 (2001).
[38] V. I. Anisimov, et al., Phys. Rev. B **71**, 125119 (2005).
[39] G. Keller, K. Held, V. Eyert, D. Vollhardt, and V. I. Anisimov, Phys. Rev. B **70**, 205116 (2004).
[40] D. Vollhardt, K. Held, G. Keller, R. Bulla, T. Pruschke, I. A. Nekrasov, and V. I. Anisimov, J. Phys. Soc. Jpn. **74**, 136 (2005).
[41] M. S. Laad, L. Craco, and E. Muller-Hartmann, Phys. Rev. Lett. **91** (2003).
[42] G. Kresse, S. Surnev, J. Schoiswohl, and F. P. Netzer, Surf. Sci. **555**, 118 (2004).
[43] V. V. Ivanovskaya, A. N. Enyashin, and A. L. Ivanovskii, Mendeleev Commun. **13**, 5 (2003).
[44] V. V. Ivanovskaya, A. N. Enyashin, A. A. Sofronov, Y. N. Makurin, N. I. Medvedeva, and A. L. Ivanovskii, Solid State Commun. **126**, 489 (2003).
[45] A. C. Santulli, et al., Phys. Chem. Chem. Phys. **11**, 3718 (2009).
[46] P. Hohenberg and W. Kohn, Phys. Rev. B **136**, B864 (1964).
[47] W. Kohn and L. J. Sham, Phys. Rev. **140**, 1133 (1965).
[48] J. M. Soler, E. Artacho, J. D. Gale, A. Garcia, J. Junquera, P. Ordejon, and D. Sanchez-Portal, J. Phys.-Condes. Matter **14**, 2745 (2002).
[49] N. Troullier and J. L. Martins, Phys. Rev. B **43**, 1993 (1991).
[50] W. R. Robinson, Acta Cryst. B **31**, 1153 (1975).
[51] L. F. Mattheiss, J. Phys.: Condens. Matter **6**, 6477 (1994).
[52] V. Eyert, U. Schwingenschlögl, and U. Eckern, Europhys. Lett. **70**, 782 (2005).
[53] J. Schoiswohl, M. Sock, S. Surnev, M. G. Ramsey, F. P. Netzer, G. Kresse, and J. N. Andersen, Surf. Sci. **555**, 101 (2004).
[54] J. Schoiswohl, S. Surnev, F. P. Netzer, and G. Kresse, J. Phys.: Condens. Matter **18**, R1 (2006).
[55] M. Schindler, F. C. Hawthorne, and W. H. Baur, Chem. Mater. **12**, 1248 (2000).
[56] F. J. Szalkowski and G. A. Somorjai, Journal of Chemical Physics **56**, 6097 (1972).
[57] K. B. Lewis, S. T. Oyama, and G. A. Somorjai, Surface Science **233**, 75 (1990).

[58] See Supplementary Information at URL to be inserted by the publihser for a discussion about discussions and figures concerning theoretical methodology, constructs, electronic structure, surface terminations, and structural characterization of the nanowires we have presented in this work.